



# Non-destructive estimation of spatially varying thermal conductivity in 3D objects using boundary thermal measurements

Sohail R. Reddy\*, George S. Dulikravich, S.M.Javad Zeidi

Department of Mechanical and Materials Engineering, MAIDROC Laboratory, Florida International University, 10555 W. Flagler St., Miami, FL 33174, USA

## ARTICLE INFO

### Article history:

Received 18 October 2016

Received in revised form 17 February 2017

Accepted 11 May 2017

Available online xxx

### Keywords:

Non-destructive testing

Inverse problems

Parameter identification

Minimization

## ABSTRACT

A methodology for non-destructive, accelerated inverse estimation of spatially varying material properties using only boundary measurements is presented. The spatial distribution of diffusion coefficient in 3D solid object is determined by minimizing the sum of the least-squares difference between measured and calculated values. The forward problem is solved using the finite volume and finite element methods, both of which were compared against analytical solution. The inverse problem was solved using an optimization technique to minimize the sum of the least-square errors. The non-destructive estimation was accelerated by the use of surrogate models to solve the forward problem. The presented methodology is applied to measurements containing varying levels of noise. Finally, it is used to detect both the location, size and shape of a subdomain within a solid object and material property of the subdomain material.

© 2016 Published by Elsevier Ltd.

## 1. Introduction

In many practical problems, physical properties of the material of an arbitrarily shaped three-dimensional object varies spatially, that is, throughout that object. Non-destructive methods that require only boundary measurements of the field variables to determine parameters defining the spatial distribution of the physical property of the material within the domain are needed.

The material properties such as thermal conductivity, electric permittivity, magnetic permeability, and concentration diffusivity, influence the spatial variation of the field quantities such as temperature, electric field potential, magnetic field potential, diffusion of non-reacting particles in a solid. These field problems can be modeled by an elliptic partial differential equation governing the steady-state diffusion of the field variable  $\phi = \phi(x, y, z)$ .

$$\nabla \cdot (\lambda \nabla \phi) = 0 \quad (1)$$

where  $\lambda = \lambda(x, y, z)$  is the diffusion coefficient. Using this mathematical model, the question to answer becomes: Using the boundary values of the field function,  $\phi$ , or its normal derivatives on the boundary of the solid, how can the spatial distribution of the diffusion coefficient  $\lambda$  be determined throughout the arbitrarily shaped solid object?

In the case of a forward or analysis problem, Eq. (1) can be numerically integrated inside the arbitrarily shaped three-dimensional

object using finite element or finite volume methods for a known distribution of  $\lambda$  and Dirichlet or Neumann boundary conditions.

In the case of an inverse problem, the spatial distribution of  $\lambda$  is not known and is to be determined iteratively. Non-destructive determination of the diffusion coefficient requires measured boundary values of  $\phi = \phi(x, y, z)$  and/or the measured values of the normal derivative of  $\phi = \phi(x, y, z)$  on the boundary of the solid object [1–3].

A variety of analytical, statistical, numerical and algorithmic approaches have been used by researchers to inversely determine spatially varying thermal conductivity in solid objects [4–10]. For example, Rodrigues et al. [6] and Naveira-Cotta et al. [7] determined non-isotropic thermal conductivity from the over-specified thermal boundary conditions using Bayesian statistics employing Kalman filter or non-linear filters. Fu et al. [8], Gu et al. [9] and Chen et al. [10] identified anisotropic thermal conductivity in 2D and 3D media. It should be pointed out that all of these methodologies focused on determining constant coefficients in a tensor representation of thermal conductivity. None of these works, however, address estimation of the more general spatially varying thermal conductivity.

However, an entirely different and computationally efficient approach to inverse determination of spatially varying physical properties of solid media is based on a combination of a field analysis algorithm (using finite volume, finite element, finite difference, radial basis function, etc.) or experimental data, and an accurate, fast and robust minimization algorithm [11–13] capable of avoiding local minima. This paper demonstrates extension of the inverse parameter identification methodology from two-dimensional arbitrarily shaped objects [14,15] to three-dimensional arbitrarily shaped objects with known outer geometry and possible internal inclusions.

The challenging inverse problem of determination of spatial distribution of diffusion coefficient in an arbitrarily shaped three-dimensional object is somewhat more tractable if  $\lambda = \lambda(x, y, z)$  is known to

\* Corresponding author.

Email addresses: [sredd001@fiu.edu](mailto:sredd001@fiu.edu) (S.R. Reddy); [dulikrav@fiu.edu](mailto:dulikrav@fiu.edu) (G.S. Dulikravich); [szeid001@fiu.edu](mailto:szeid001@fiu.edu) (S.M.Javad Zeidi)

vary as a function of  $x, y, z$  according to an analytic function defined by a number of unknown parameters. The easiest and the most versatile method for solving this inverse problem is minimization of the properly scaled sum of squares of differences between the computed  $\phi$  or  $\partial\phi/\partial n$  values on the boundaries subject to chosen values of these parameters, and the measured  $\phi$  or  $\partial\phi/\partial n$  values on the boundaries. In this case, these unknown parameters need to be iteratively optimized to give an accurate match between the calculated and the measured boundary values of  $\phi$  or  $\partial\phi/\partial n$ . This method will be now presented on sequence of examples dealing with inverse determination of parameters governing spatial variation of one of the most common diffusion coefficients  $\lambda = \lambda(x, y, z)$  known as thermal conductivity,  $k(x, y, z)$ .

It should be pointed out that an unrelated inverse problem is inverse determination of thermal conductivity as a function of temperature (not space) which can be efficiently and accurately solved with the use of Kirchhoff's transformation [16].

## 2. Validation of numerical solvers for forward problem

With advances in additive manufacturing, it is now possible to create three-dimensional objects that feature spatially varying thermo-physical properties. Also, it can often become imperative to non-destructively determine the thermo-physical properties of such objects.

The previously posed inverse problem, when applied to the thermal diffusion problems, can be stated as: *For a specified temperature/heat flux distribution on the boundaries of a solid object, what should be the spatial variation of thermal conductivity in this domain that will create such temperature/heat flux distribution at the boundaries?*

As previously mentioned, the methodology in this work uses a least-squares minimization technique that requires the temperature and/or heat flux to be calculated at the boundary of the domain. This was done by numerically integrating Eq. (1) using the finite volume method in ANSYS Fluent [17] software package. The spatial variation of thermal conductivity was incorporated using a User-Defined Function (UDF) in this analysis software package.

In this inverse parameter identification method, it is necessary to solve the forward (analysis) problem several times. For this reason, the accuracy of the numerical integration code needs to be verified. The accuracy verification was performed against analytical solutions. One such analytical solution test case can be formulated as a three-dimensional cube  $x \in [0, 1]$ ,  $y \in [0, 1]$ ,  $z \in [0, 1]$  with the distribution of thermal conductivity defined by

$$k(x, y, z) = [(A + x)(B + y)(C + z)]^{1-n} \quad (2)$$

Here,  $A, B, C$  and  $n$  are arbitrary parameters. The corresponding analytical solution for the temperature field then has the general form

$$T(x, y, z) = (A + x)^n + (B + y)^n + (C + z)^n \quad (3)$$

The accuracy verification was performed by solving Eq. (1) in a cube subject to Dirichlet conditions specified in Table 1 where  $A = B = C = 1.0$  and  $n = 2$ . Equation (1) was solved using ANSYS Fluent [17] with UDF on a computational grid of  $62 \times 62 \times 62$  grid cells.

Fig. 1 shows the analytical distribution of thermal conductivity defined by Eq. (2), analytical temperature field, computed temperature field and the relative error between the computed and analytical

**Table 1**

Dirichlet boundary conditions, when  $A = B = C = 1.0$  and  $n = 2$ .

	Location	Dirichlet boundary conditions
East boundary	$x = 1.0$	$T(1, y, z) = 4 + (1 + y)^2 + (1 + z)^2$
West boundary	$x = 0.0$	$T(0, y, z) = 1 + (1 + y)^2 + (1 + z)^2$
North boundary	$y = 1.0$	$T(x, 1, z) = 4 + (1 + x)^2 + (1 + z)^2$
South boundary	$y = 0.0$	$T(x, 0, z) = 1 + (1 + x)^2 + (1 + z)^2$
Top boundary	$z = 1.0$	$T(x, y, 1) = 4 + (1 + x)^2 + (1 + y)^2$
Bottom boundary	$z = 0.0$	$T(x, y, 0) = 1 + (1 + x)^2 + (1 + y)^2$

temperature fields subject to boundary conditions in Table 1. It can be seen that the maximum relative error is 0.015%. It shows that the proposed numerical method is capable of producing accurate results and therefore can be used for the proposed inverse problem method.

## 3. Inverse problem solution methodology

The solution of the inverse problem results in the determination of parameters defining thermal conductivity variation throughout the domain. This methodology minimizes the sum of normalized least-squares differences between measured and calculated boundary values of the field variable by iteratively adjusting these parameters. Let us refer to temperature or temperature gradient on the boundaries obtained from experiments or analytical solution as "measured" values. Let us refer to temperature or temperature gradient on the boundaries obtained from the solution of the forward problem with guessed values of the parameters defining spatial distribution of thermal conductivity as "calculated" values. Then the functional to minimize becomes

$$J = \sum_{\partial S} \left[ \left( T_j^{calc} - T_j^{meas} \right) / \left( T_j^{meas} + \varepsilon \right) \right]^2 \quad (4)$$

where  $\varepsilon$  is a very small positive number of the order  $1.0E-06$  (to prevent division by zero when measured boundary temperature is zero) and summation is performed over  $\partial S$ , the boundary of the arbitrarily shaped solid object.

The minimization of Eq. (4) was performed using a hybrid of particle swarm and Broyden-Fletcher-Goldfarb-Shanno (BFGS) algorithms [11–13]. The optimizer iteratively modifies the parameters defining the distribution of thermal conductivity in the forward problem during minimization of the  $J$  functional. A hybrid optimization algorithm was chosen because it is highly reliable and fast. That is, single-objective optimization algorithms based on gradient search have good convergence rates, but their search will often terminate in the nearest feasible minimum instead in the global minimum. Non-gradient population-based optimization algorithms converge at a slower rate, but are able to successfully converge to the immediate vicinity of the global minimum. A typical hybrid optimizer [11–13] is a set of one or more of the gradient-based optimizers and one or more of the population-based optimizers, with an automatic switching logic among these algorithms after every iteration (or population generation) in order to maximize the overall convergence rate and avoid local minima. In this work, instead of automatically switching back-and-forth between the BFGS and the particle swarm optimizers, the population based algorithm was used exclusively until the search converge to the vicinity of the global minimum (when the convergence rate became very low) and then switched [18] to exclusively using BFGS fast gradient-based optimizer to quickly converge to the actual global minimum point.

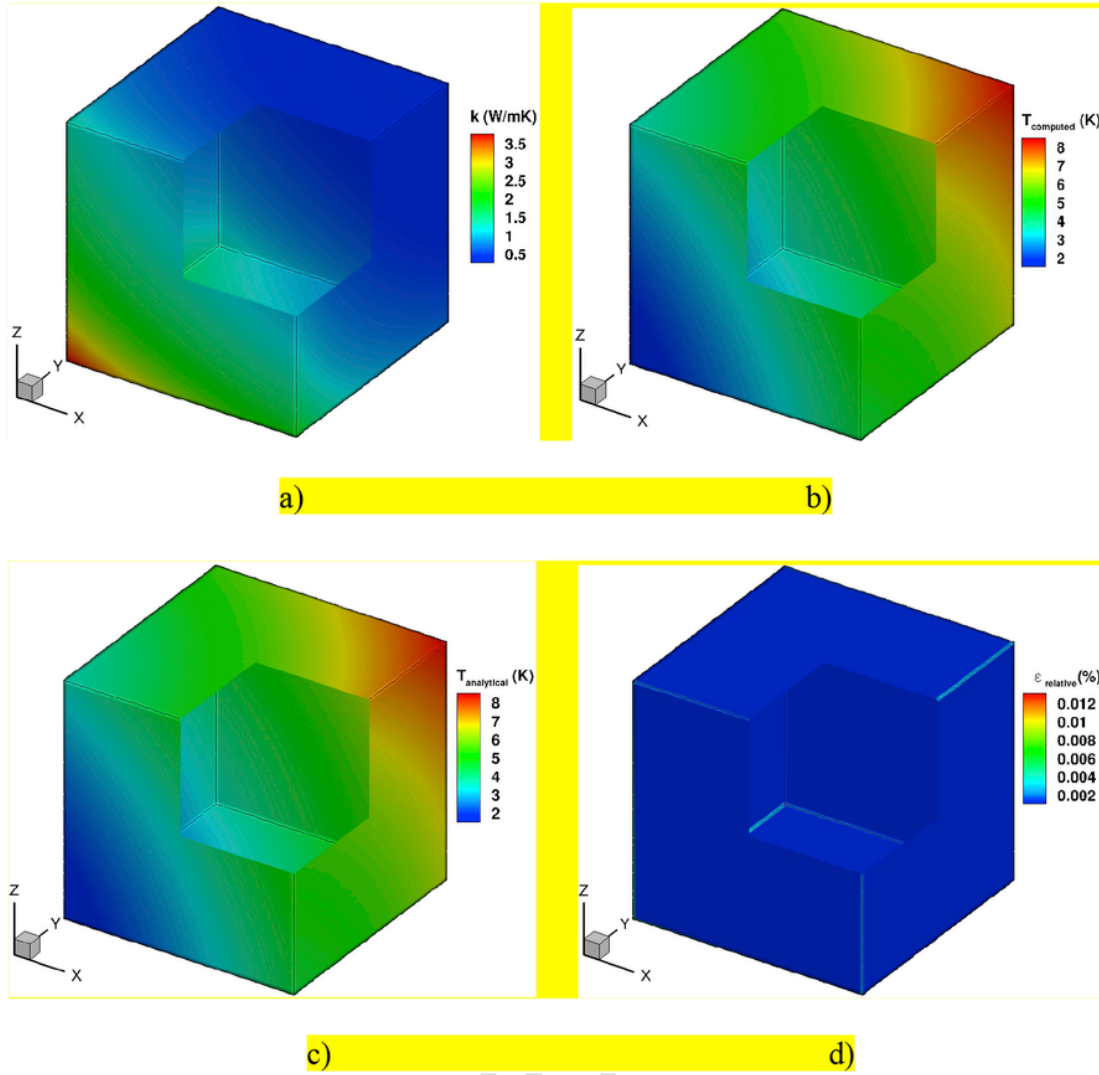


**Fig. 1.** Distribution of: a) analytical thermal conductivity, b) analytical temperature field given by Eq. (3), c) calculated temperature field using ANSYS Fluent and analytical thermal conductivity given by Eq. (2), and d) relative error of temperature computed using ANSYS Fluent.

In certain cases, it can be computationally expensive to compute the forward problem especially when using a very fine computational grid. The forward problem needs to be solved a large number of times, each time for different guessed values of thermal conductivity parameters. Thus, it is more economical to replace the finite volume or the finite element solver with a less accurate, but much faster surrogate model. For this reason, a response surface [12,13] was created for the  $J$  functional and then used to extremely quickly predict the forward problem solutions for any guessed values of the parameters defining thermal conductivity spatial variation. The response surface of the  $J$  functional was created by interpolating  $J$  values calculated using high fidelity ANSYS analyses corresponding to a relatively small set of randomly distributed values of the unknown thermal conductivity parameters created using Sobol's algorithm [19]. The entire methodology is summarized in Fig. 2.

All simulations were run on a single core of an Intel Xeon CPU E5-4620. Each finite volume analysis took approximately 15 s, while the response surface was constructed in less than 10 s. Once the response surface was constructed using the  $J$  functional values from the analysis runs, the optimizer, when coupled with the response surface, took approximately 20–30 s for each case to minimize Eq. (4).

## 4. Numerical results

### 4.1. Case 1: inverse determination of smoothly varying thermal conductivity

The proposed inverse problem solution methodology was validated for a simple cube. The thermal conductivity was defined by Eq. (2), in a cube where  $x \in [0, 1]$ ,  $y \in [0, 1]$  and  $z \in [0, 1]$ , and subjected to boundary conditions defined by Eq. (3) where the parameters were  $A = 1.25$ ,  $B = 1.34$ ,  $C = 3.20$  and  $n = 2$ . The east, west, north, south and top faces were subject to Neumann boundary conditions, while the bottom face was subjected to Dirichlet boundary condition. The Neumann boundary condition can be computed by analytically differentiating Eq. (3).

The “calculated” values were obtained using ANSYS Fluent and guessed values of  $A$ ,  $B$  and  $C$ , while the “measured” values were obtained from the analytical solution Eq. (3). The three-dimensional response surface was created using Shepard's K-Nearest algorithm [18] that was supported by 30 values of the  $J$  functional obtained using 30 guessed sets of parameters  $A$ ,  $B$  and  $C$  in Eq. (2). In this example, the

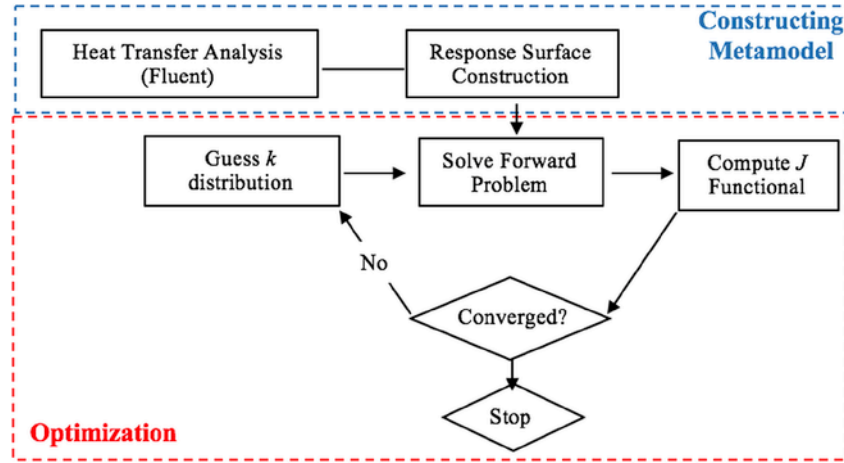


Fig. 2. Inverse problem methodology.

hybrid particle swarm-BFGS optimizer [18] was coupled with the three-dimensional response surface to minimize the  $J$  functional.

Table 2 shows converged value of the parameters  $A$ ,  $B$  and  $C$  that best minimized the  $J$  functional. Relative error of the inversely determined parameters was less than 1%. The maximum computing time required to converge the three unknown parameters was less than 45 min. This includes times to construct the response surface as well as the optimization. In previous work dealing with two-dimensional problems only [14,15], which did not use a response surface, the computing times were more than 10 h.

Fig. 3 shows the distribution of analytical thermal conductivity, analytical temperature field, converged distribution of thermal conductivity and the relative error between analytical and converged distribution of thermal conductivity. It shows that the difference between the analytical thermal conductivity and converged thermal conductivity is less than 0.01%, thereby validating the proposed methodology for inverse determination of spatially varying thermal conductivity.

#### 4.2. Case 2: determination of sharp gradient thermal conductivity

It has been shown that the proposed methodology is able to determine the distribution of smoothly varying thermal conductivity when it follows a simple function. Its ability to determine sharply varying 3D distribution of thermal conductivity is investigated. In this test case, the “measured” solution is no longer obtained using the analytical solution, but rather by using analysis from COMSOL software [20].

Table 2

Case 1: Converged values of coefficients for  $n = 2$ .

	$A$	$B$	$C$
Exact	1.250	1.340	3.20
Inversely Determined	1.248	1.337	3.20
Relative error	0.8%	0.22%	0%

The thermal conductivity was assumed to have the form

$$k(x, y, z) = \frac{(k_{\max} + k_{\min})}{2} + (k_{\max} - k_{\min}) \left[ \frac{x}{x_{\max}} - \frac{A}{2\pi} \sin^D(2\pi x) \right] \left[ \frac{y}{y_{\max}} - \frac{B}{2\pi} \sin^E(2\pi y) \right] \times \left[ \frac{z}{z_{\max}} - \frac{C}{2\pi} \sin^F(2\pi z) \right] \quad (5)$$

The “measured” solution was obtained by solving Eq. (1) using the distribution of thermal conductivity given in Eq. (5) (with boundary conditions given in Table 4) using the finite element method in COMSOL. When solving inverse problems, one must avoid the so called “inverse crime”. This is because in a numerical study, the inverse problem will converge exactly to the measurements if the “measurements” were obtained using the same analysis code as that used in the inverse problem. To avoid this, two different solvers must be used; one to obtain the “measurements” (COMSOL) and another (ANSYS) to solve the forward problem. It should be pointed out that, once the response surface is used to solve the forward problem, this inverse crime issue is avoided altogether as the response surface is a very crude but efficient approximation to the  $J$  functional. It does not know anything about the physics of the heat transfer problem. In Case 1, the “measurements” were given as an analytic solution instead of been simulated by any computer code. In other cases, the “measurements” were generated using COMSOL, while forward solutions needed for the generation of the response surface were generated using ANSYS. The  $J$  functional was then calculated using these “measured” and “calculated” values.

An eight-dimensional response surface was created using 80 support points by means of the Shepard’s K-Nearest algorithm [18]. The optimizer was then coupled with this response surface to find values of the eight parameters that best minimized the  $J$  functional. The range for each variable that the optimizer was allow to search is given in Table 3.

Table 4 shows the boundary conditions applied to the cube, where  $q$  is the heat flux. The  $J$  functional was constructed using the temperature value on the east, west, north, south and top boundaries. The computational grid has the same size as the one used in Case 1 study.

As is often the case, the “measured” values that are obtained from an experiment often have some level of noise. To account for this,

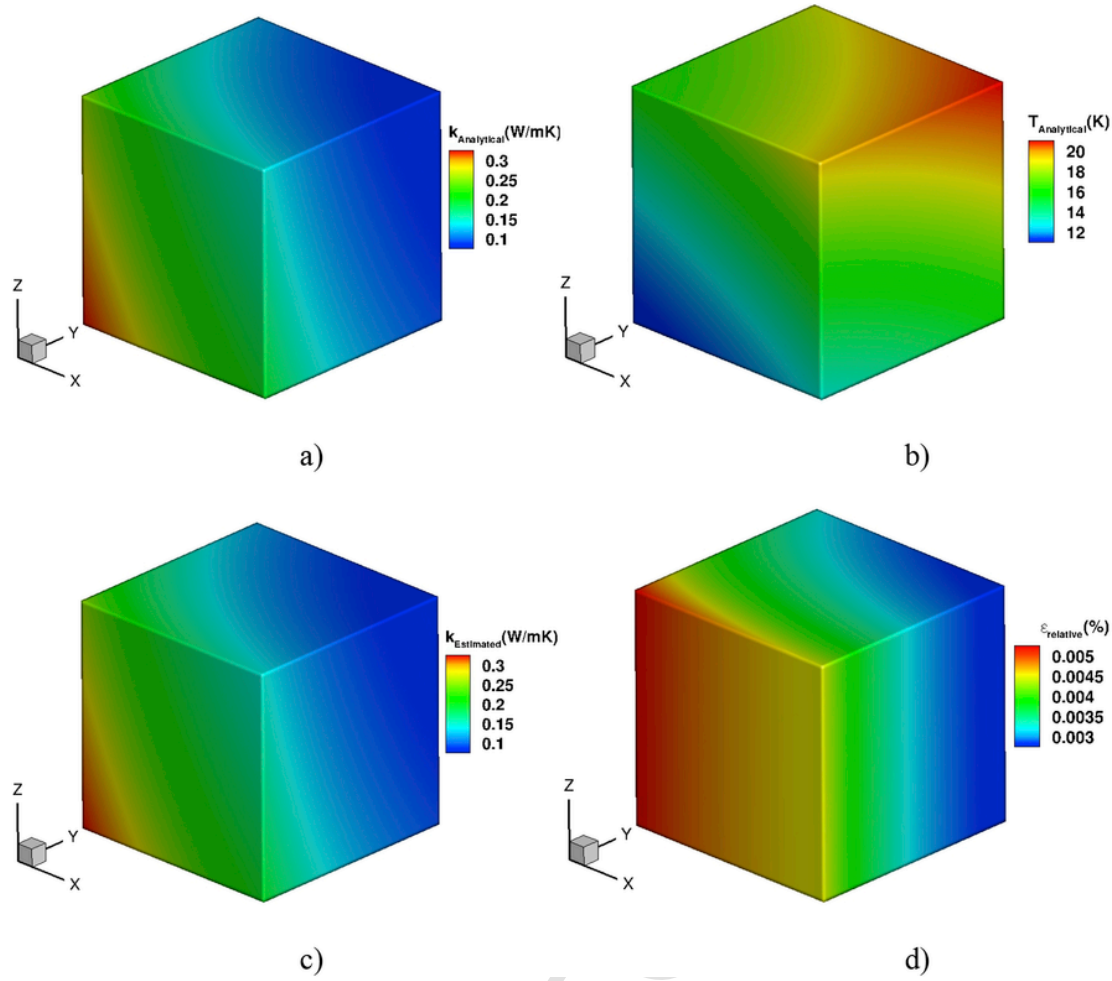


**Fig. 3.** Case 1 - Distribution of: a) analytical thermal conductivity, b) analytical temperature distribution, c) inversely determined thermal conductivity, and d) relative error between exact and estimated thermal conductivity.

**Table 3**

Case 2 - Allowable range and step size for each unknown parameter in Eq. (5).

	$k_{\min}$	$k_{\max}$	$A$	$B$	$C$	$D$	$E$	$F$
Min	100	1000	0	0	0	1	1	1
Max	500	6000	1.0	1.0	1.0	100	100	100
Step Size	10	10	0.01	0.01	0.01	1	1	1

**Table 4**

Case 2 - Boundary conditions, when  $k_{\min} = 200$ ,  $k_{\max} = 5000$ ,  $A = B = C = 0.85$  and  $D = E = F = 50$ .

Boundary conditions	
East boundary	$q(1, y, z) = 10 \times k(1, y, z)$
West boundary	$q(0, y, z) = 10 \times k(0, y, z)$
North boundary	$q(x, 1, z) = 10 \times k(x, 1, z)$
South boundary	$q(x, 0, z) = 400 \times k(x, 0, z)$
Top boundary	$q(x, y, 1) = 600 \times k(x, y, 1)$
Bottom boundary	$T(x, y, 0) = 85 \text{ K}$

noise was added to the “measured” values obtained from COMSOL. The noise model used was additive white Gaussian [21]. The “measured” values were perturbed by a noise-signal ratio of 1%, 3%, 5% and 10%. In reality, the actual Type J, K, E, T thermocouples and resistance temperature detectors (RTDs) all have a maximum error of approximately 1% [22].

Table 5 shows the values of the converged six parameters in Eq. (5) with varying level of noise. It is evident that the inverse problem methodology is also able to determine a highly non-linear distribution of the diffusion coefficient. The table also shows the values of the  $J$  functional when the analytical values of the six parameters are used to solve Eq. (1) and perturbed “measured” values are used to construct the  $J$  functional. It can be seen that the  $J$  functional rapidly increases for noise levels greater than approximately 2%.

Fig. 4 shows the distribution of converged thermal conductivity for varying levels of noise in “measured” thermal boundary conditions. Good convergence can be seen for noise levels up to 3%. This shows that the methodology is able to inversely determine even a sharp gradient distribution of thermal conductivity for high measure-

**Table 5**

Case 2: Converged values of coefficients, and  $J$  functional with randomly perturbed boundary values.

	$k_{\min}$	$k_{\max}$	$A$	$B$	$C$	$D$	$E$	$F$	$J_{\text{Analytical}}$
Analytical	200	3000	0.85	0.85	0.85	50	50	50	—
$\epsilon_{\text{meas}} = 0\%$	200	3000	0.85	0.85	0.85	50	50	50	3E-8
$\epsilon_{\text{meas}} = 1\%$	200	3000	0.85	0.85	0.85	50	50	50	8E-6
$\epsilon_{\text{meas}} = 3\%$	200	3000	0.85	0.85	0.85	50	50	50	43.3
$\epsilon_{\text{meas}} = 5\%$	410	4210	0.83	0.70	0.52	95	21	34	2.8E7
$\epsilon_{\text{meas}} = 10\%$	340	4910	0.32	0.82	0.71	85	4	35	5.9E6



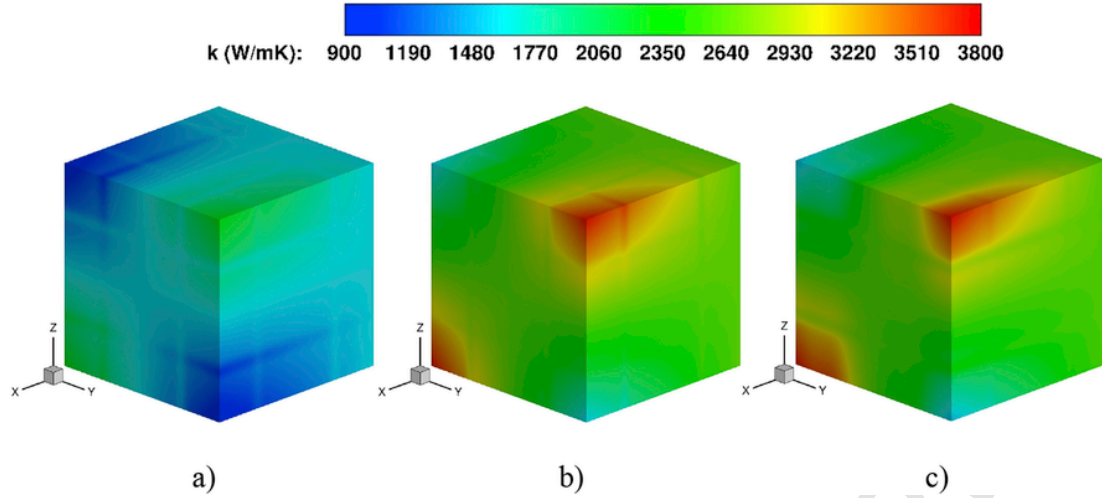


Fig. 4. Converged thermal conductivity for: a)  $\epsilon_{meas} = 0\%$ ,  $\epsilon_{meas} = 1\%$ ,  $\epsilon_{meas} = 3\%$ , b)  $\epsilon_{meas} = 5\%$ , c)  $\epsilon_{meas} = 10\%$ .

ment noise levels, considering the maximum noise experienced by an actual thermocouple is less than 1%.

Fig. 5 shows the relative error of the converged calculated distribution of thermal conductivity and its analytical distribution. The relative error is zero for noise levels below 5%. It can be seen that the distribution of the thermal conductivity is still predicted relatively accurately despite the large noise present in the measured data.

#### 4.3. Case 3: determination of sharp gradient thermal conductivity in arbitrary domain

In the previous two cases, a cube was used to demonstrate the efficiency of the proposed methodology. However, the proposed methodology can also be applied to arbitrary shaped domains. In this section, an arbitrary three-dimensional configuration featuring no planar symmetry or axis-symmetry is used (Fig. 6). The parametric

equations defining this geometry are given by Lamé curves as

$$r = r_0 - A \cos(3\theta), \quad \text{where } r_0 = 1, A = 0.2, \quad 0.0 \leq \theta \leq 2\pi$$

$$\left[ \frac{x-0.4}{0.2} \right]^2 + \left[ \frac{y-0.2}{0.2} \right]^2 = 1, \quad \left[ \frac{x+0.5}{0.1} \right]^4 + \left[ \frac{y-0.2}{0.3} \right]^4 = 1,$$

$$\left[ \frac{x-0.1}{0.4} \right]^2 + \left[ \frac{y+0.5}{0.3} \right]^2 = 1$$

Fig. 6 shows the arbitrary multiply-connected geometry defined by Eq. (6). Each of the four boundaries is revolved by a different angle  $\sigma$  about the axis which is offset by 2 m from the origin. This ensures there is neither a planar symmetry nor axisymmetry.

The assumed distribution of thermal conductivity is again given by Eq. (5), where the eight parameters are given in Table 5. The governing Eq. (1) was subject to boundary conditions given in Table 6. The “measured” values were once again obtained using COMSOL. The  $J$  functional was constructed using temperature values on bound-

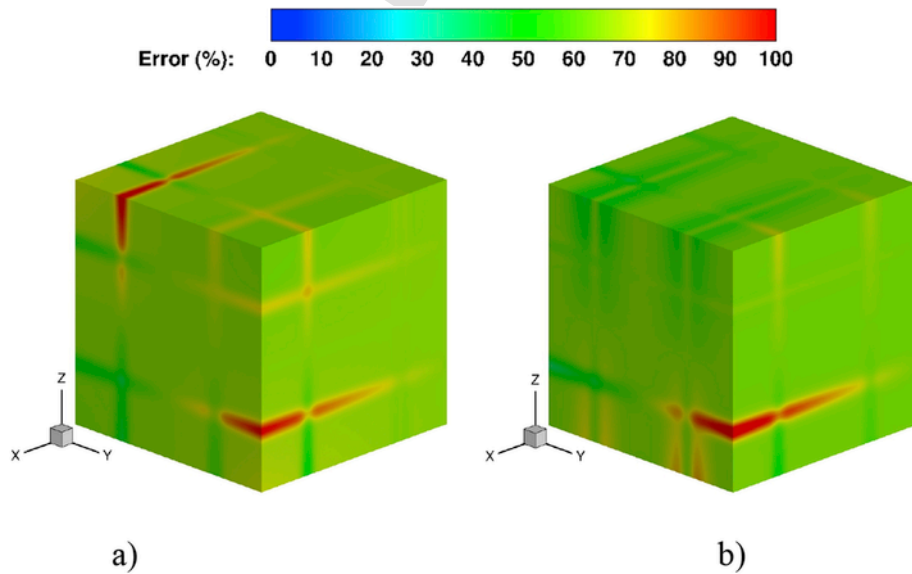
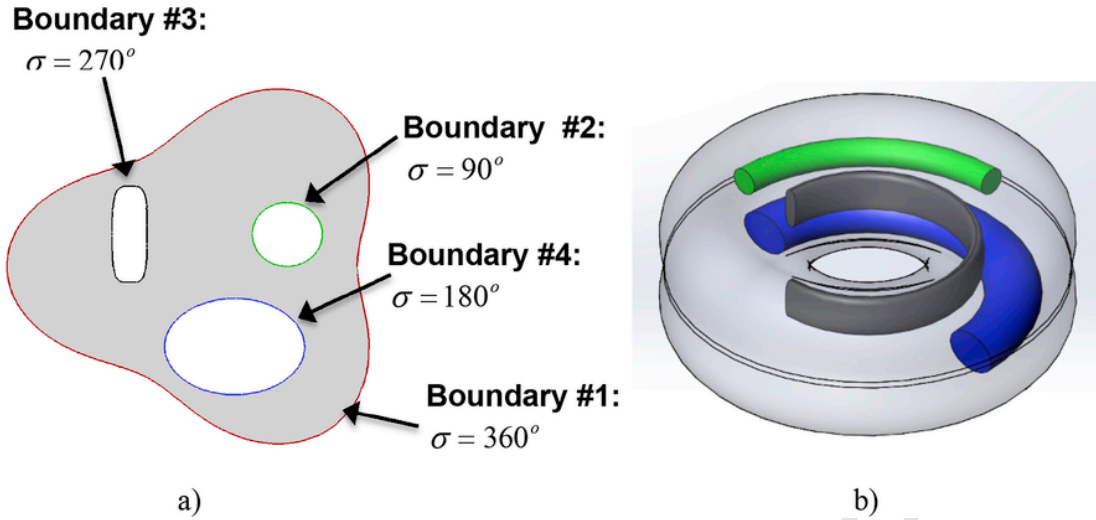


Fig. 5. Relative error in Case 2 between analytical and converged distribution of thermal conductivity for: a)  $\epsilon_{meas} = 5\%$  and b)  $\epsilon_{meas} = 10\%$ .



**Fig. 6.** Case 3: Arbitrary three-dimensional geometry example: a) vertical cross section plane of a torus showing cross-sections of three cavities, and b) an isometric translucent view of the complete 3D torus with three cavities.

**Table 6**

Case 3: Boundary conditions when  $k_{\min} = 420$ ,  $k_{\max} = 3160$ ,  $A = 0.44$ ,  $B = 0.62$ ,  $C = 0.33$  and  $D = 34$ ,  $E = 42$ ,  $F = 21$ .

	Boundary conditions
Boundary #1	$T = 330 \text{ K}$
Boundary #2	$q = 30000 \times k(x, y, z)$
Boundary #3	$q = 60000 \times k(x, y, z)$
Boundary #4	$q = 40000 \times k(x, y, z)$

aries #2, #3 and #4. A total of 80 support points (80 numerical analyses with different values of the eight parameters) were used to create the response surface again by means of the Shepard's K-Nearest algorithm [18].

Table 7 shows the converged values of the eight parameters in Case 3 under varying noise levels for the three-dimensional configuration given in Fig. 6. It can again be seen that the  $J$  functional grows exponentially for noise levels greater than approximately 1.5%.

Fig. 7 shows the converged distribution of thermal conductivity for the Case 3. It can be seen that again for noise levels up to 3%, the proposed methodology is able to accurately determine the distribution of diffusion coefficient.

Fig. 8 shows the relative error between the converged distribution of thermal conductivity and its analytical distribution. It was observed that a sensitive distribution of assumed thermal conductivity as in Eq. (5) leads to a highly non-linear and highly multimodal objective function topology featuring sharp gradients near the global minimum. For this reason a powerful and robust optimizer is needed to avoid the local minima. An improvement in accuracy could be expected when using strictly high fidelity analyses instead of a relatively low fidelity response surface metamodel.

**Table 7**

Case 3: Converged values of the six parameters and  $J$  functional with randomly perturbed boundary values.

	$k_{\min}$	$k_{\max}$	$A$	$B$	$C$	$D$	$E$	$F$	$J_{\text{Analytical}}$
Analytical	420	3160	0.44	0.62	0.33	34	42	21	
$\epsilon_{\text{meas}} = 0\%$	420	3160	0.44	0.62	0.33	34	42	21	2E-8
$\epsilon_{\text{meas}} = 1\%$	420	3160	0.44	0.62	0.33	34	42	21	2E-6
$\epsilon_{\text{meas}} = 3\%$	420	3160	0.44	0.62	0.33	34	42	21	10.9
$\epsilon_{\text{meas}} = 5\%$	450	4860	0.83	0.47	0.25	95	95	49	260
$\epsilon_{\text{meas}} = 10\%$	450	4860	0.83	0.47	0.25	95	95	49	5.5E6

It can be reported that the optimizer took longer to converge in Case 2 and in Case 3 than in Case 1, due to the highly non-linear and sensitive assumed distribution of thermal conductivity. With the use of high fidelity finite element or finite volume for each of the analyses, the computing time would have been an order of magnitude longer.

#### 4.4. Case 4: determination of subdomains within solid objects

Using this general approach, it is possible to detect subdomains (one material subdomain imbedded within another material domain) by minimizing the  $J$  functional. This will be demonstrated on a simple cube made of silicon with an embedded subdomain of gold. It will be assumed that the subdomain general shape inside the cube is defined by a modified Lamé super-ellipsoid whose location, size and shape and its thermal conductivity are unknown.

$$f(x, y, z) = \left[ \left( \frac{x - x_0}{A} \right)^{2/n_2} + \left( \frac{y - y_0}{B} \right)^{2/n_2} \right]^{n_2/n_1} + \left( \frac{z - z_0}{C} \right)^{2/n_1} = 1 \quad (7)$$

It will also be assumed that the property of the encasing material is also unknown.

Distribution of thermal conductivity can then be assumed to have the discontinuous form

$$\begin{aligned} f(x, y, z) > 1 &\rightarrow k = k_{\text{silicon}} \\ f(x, y, z) \leq 1 &\rightarrow k = k_{\text{gold}} \end{aligned} \quad (8)$$

The “measured” values of thermal boundary conditions were obtained by means of the finite element method using the exact values (Table 8) of thermal conductivities, geometry definition parameters used in Eq. (7) and thermal boundary conditions given in Table 4. A total of 110 support points were used to create a response surface using the Shepard's K-Nearest algorithm. To allow for the accurate

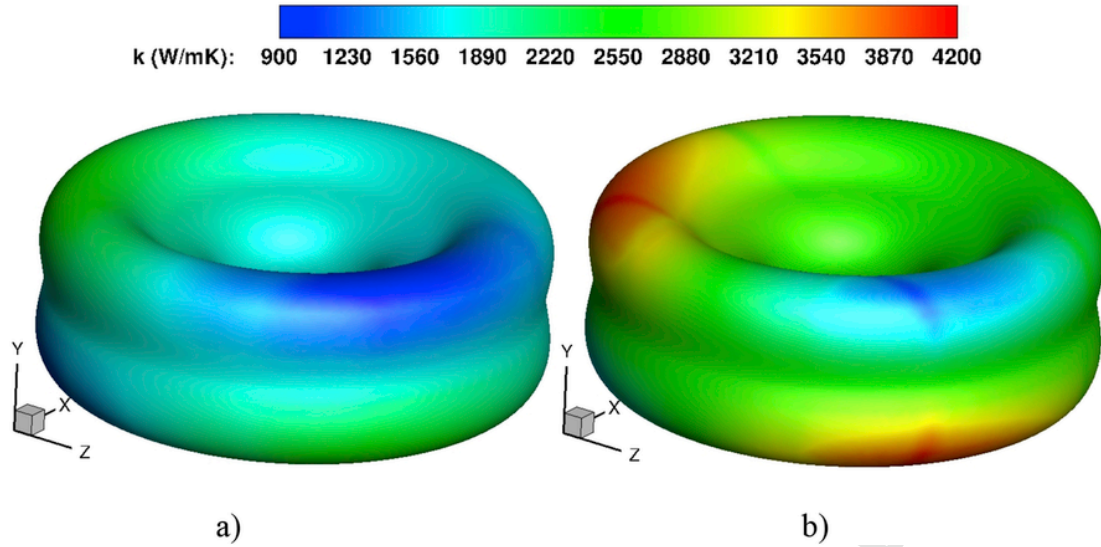


Fig. 7. Case 3 – Converged spatial distribution of thermal conductivity for: a)  $\epsilon_{meas} = 0\%$ ,  $\epsilon_{meas} = 1\%$ ,  $\epsilon_{meas} = 3\%$ , and b)  $\epsilon_{meas} = 5\%$ ,  $\epsilon_{meas} = 10\%$ .

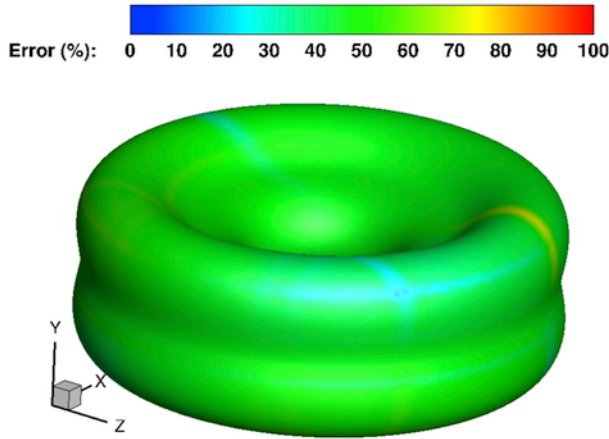


Fig. 8. Case 3 - Relative error between analytical and converged thermal conductivity for  $\epsilon_{meas} = 5\%$  and  $\epsilon_{meas} = 10\%$ .

Table 8

Case 4 - Converged values of ten parameters in Eq. (8) with randomly perturbed thermal boundary values.

	$k_{silicon}$	$k_{gold}$	$x_o$	$y_o$	$z_o$	$A$	$B$	$C$	$n_1$	$n$
Analytical	149	385	-0.5	0.0	-0.15	0.25	0.25	0.25	0.5	1
$\epsilon_{meas} = 0\%$	149	385	-0.5	0.0	-0.15	0.25	0.25	0.25	0.5	1
$\epsilon_{meas} = 1\%$	149	385	-0.5	0.0	-0.15	0.26	0.24	0.245	0.5	1
$\epsilon_{meas} = 3\%$	149	385	-0.56	0.0	-0.15	0.27	0.24	0.245	0.61	1

analysis of vastly diverse shapes, the computational grid resolution was increased to  $110 \times 110 \times 110$ .

The ten converged parameters from Eq. (8) for varying levels of noise in the “measured” thermal boundary conditions are shown in Table 8. It can be seen that the optimizer was able to accurately determine the location, size and shape of the subdomain and thermal conductivities of the materials in the two domains.

Fig. 9 shows the location and the shape of the identified subdomain. It can be seen that the location is exact for all three cases. The assumed distribution of thermal conductivity was relatively sensitive with respect to each of the ten variables.

This demonstrated that this non-destructive evaluation method is also capable of identifying sizes, shapes and locations of imbedded subdomains and discontinuous distribution of diffusion coefficient in such subdomains.

The number of parameters that can be determined using this methodology can be much higher. For example,

The accuracy of this methodology is dependent on the accuracy of the forward problem solver (which was verified), the assumed function distribution (which can be overcome using a product of two or three Fourier series), the accuracy of the response surface generation algorithm used, and the reliability and accuracy of optimizer used to perform the minimization. It is true that for larger number of unknowns, a more powerful optimizer is needed. One such optimizer is IOSO which can cope with hundreds of unknowns. Our hybrid single-objective optimizer successfully performed on analytical problems with up to 100 design variables having different degrees of nonlinearities.

## 5. Conclusion

The continuous and discontinuous distribution of material properties within a solid object can be non-destructively determined using a minimization of a sum of the least squares between the calculated and measured boundary conditions. Numerical integration of the governing PDE was performed using the finite volume and finite element methods and was validated against analytical solution. This inverse parameter identification technique showed promising results for both a continuous and discontinuous, smoothly varying and sharply varying distribution of the diffusion coefficient in arbitrary domains. Total computing time was significantly reduced from 10 + hours to under 1 h by the use of metamodels. It was demonstrated that even a sensitive and highly non-linear distribution of the material properties can be estimated. The presented methodology was able to determine the distribution of the diffusion coefficient for boundary temperature measurement noise levels up to 3% when using response surface metamodels, which is appealing as a typical temperature measurement apparatus has a noise level of 1%. This approach to inverse identification of unknown parameters was also demonstrated as capable of accurately determining sizes, shapes and locations of subdomains and material properties in the subdomains imbedded within a



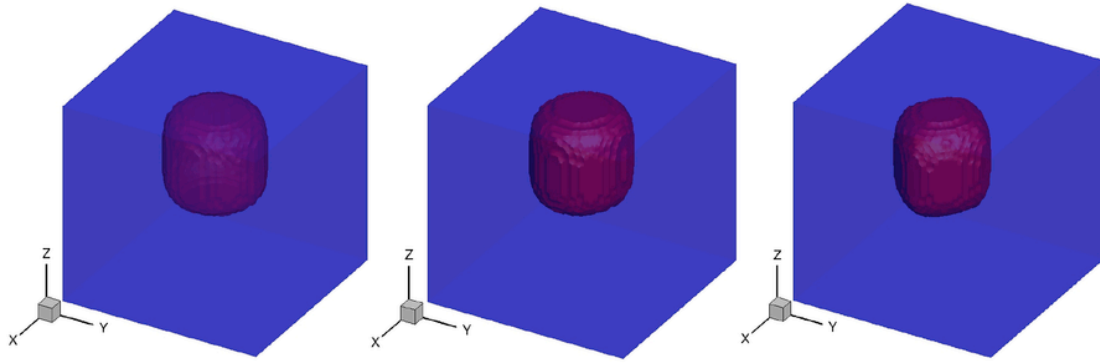


Fig. 9. Case 4 - Inversely determined location, size and shape of a subdomain containing gold for: a)  $\epsilon_{meas} = 0\%$ , b)  $\epsilon_{meas} = 1\%$ , and c)  $\epsilon_{meas} = 3\%$ .

solid object. Finally, it should be pointed out that this parameter identification method is directly applicable to determination of parameters defining spatial distributions of thermal conductivity, electric permittivity and magnetic permeability and that it is truly non-destructive. It took approximately 30 min to 1 h to obtain objective function values needed to construct the response surface. The actual construction of the response surface took less than 5 s. Once the response surface was coupled with the optimizer, the minimization process took approximately 30 s. Thus, the most computationally expensive task in this entire procedure is obtaining the objective function values needed to construct a response surface. An alternative would be to use reduced order modeling instead of the response surface approach, although both approaches require a number of high fidelity forward solutions as a starting point.

## Acknowledgement

The lead author gratefully acknowledges the financial support from Florida International University in the form of an FIU Presidential Fellowship. This work was partially supported on a National Science Foundation EAGER grant CBET-1642253 monitored by Dr. Jose Lage. The views and conclusions contained herein are those of the authors and should not be interpreted as necessarily representing the official policies or endorsements, either expressed or implied, of the US National Science Foundation or the U.S. Government. The U.S. Government is authorized to reproduce and distribute reprints for government purposes notwithstanding any copyright notation thereon.

## References

- [1] A.P. Calderón, On an inverse boundary value problem, In: Seminar on Numerical Analysis and its Applications to Continuum Physics (Rio de Janeiro 1980), Brazilian Mathematical Society, Rio de Janeiro, 1980, pp. 65–73.
- [2] S. Ciulli, M.K. Pidcock, C. Sebu, An integral equation method for the inverse conductivity problem, *Phys Lett A* 325 (3) (2004) 253–267.
- [3] M.V. Klibanov, A. Timonov, Carleman estimates for coefficient inverse problems and numerical applications, VSP, Utrecht, 2004.
- [4] J. Lee, G. Uhlmann, Determining anisotropic real-analytic conductivities by boundary measurements, *Comm Pure Appl Math* 42 (8) (1989) 1097–1112.
- [5] J. Sylvester, An anisotropic inverse boundary value problem, *Comm Pure Appl Math* 43 (2) (1990) 201–232.
- [6] F.A. Rodrigues, H.R.B. Orlando, G.S. Dulikravich, Simultaneous estimation of spatially-dependent diffusion coefficient and source term in nonlinear 1D diffusion problems, *Math Comput Simul* 66 (4–5) (2004) 409–424.
- [7] C. Naveira-Cotta, H.R.B. Orlando, R. Cotta, Combining integral transforms and Bayesian inference in the simultaneous identification of variable thermal conductivity and thermal capacity in heterogeneous media, *ASME J Heat Transf* 133 (2011) 111301–111311.
- [8] Z. Fu, W. Chen, C.-Z. Zhang, Boundary particle method for Cauchy inhomogeneous potential problems, *Inverse Probl Sci Eng* 20 (2) (2012) 189–207.
- [9] Y. Gu, W. Chen, Z.-J. Fu, Singular boundary method for inverse heat conduction problems in general anisotropic media, *Inverse Probl Sci Eng* 22 (6) (2014) 889–909.
- [10] B. Chen, W. Chen, A.H.D. Cheng, L.L. Sun, X. Wei, H. Peng, Identification of the thermal conductivity coefficients of 3D anisotropic media by the singular boundary method, *Int J Heat Mass Transf* 100 (2016) 24–33.
- [11] G.S. Dulikravich, T.J. Martin, B.H. Dennis, N.F. Foster, Multidisciplinary hybrid constrained GA optimization, In: K. Miettinen, M.M. Makela, P. Neittaanmaki, J. Periaux (Eds.), EUROGEN99-Evolutionary algorithms in engineering and computer science: recent advances and industrial applications, vol. 3, John Wiley & Sons, Jyväskylä, Finland, 1999, pp. 233–259. May 30-June.
- [12] M.J. Colaco, G.S. Dulikravich, D. Sahoo, A response surface method-based hybrid optimizer, *Inverse Probl Sci Eng* 16 (6) (2008) 717–741.
- [13] M.J. Colaco, G.S. Dulikravich, A survey of basic deterministic, heuristic and hybrid methods for single-objective optimization and response surface generation, In: Thermal measurements and inverse techniques, Taylor & Francis, New York, 2011, pp. 355–405.
- [14] M. A. Pasqualetto, M. J. Colaco, G. S. Dulikravich, H. R. B. Orlando and T. J. Martin, Inverse determination of spatially varying thermal conductivity based on boundary temperature and heat flux measurements, in: Symposium on Inverse Problems, Design and Optimization-IPDO2013, Albi, France (2013).
- [15] G.S. Dulikravich, S.R. Reddy, M.A. Pasqualetto, M.J. Colaco, H.R.B. Orlando, J. Coverston, Inverse determination of spatially varying material coefficients in solid objects, *J Inverse Ill-Posed Probl* (January 2016) <http://dx.doi.org/10.1515/jiip-2015-0057>.
- [16] T.J. Martin, G.S. Dulikravich, Inverse determination of temperature-dependent thermal conductivity using steady surface data on arbitrary objects, *ASME J Heat Transf* 122 (2000) 450–459.
- [17] ANSYS fluent 12.0, UDF manual, ANSYS Inc., [www.ansys.com](http://www.ansys.com).
- [18] Ver. 4.5.4 modeFRONTIER, software package, ESTECO, Trieste, Italy, 2014.
- [19] I.M. Sobol, Distribution of points in a cube and approximate evaluation of integrals, *U.S.S.R Comput Maths Math Phys* 7 (1967) 86–112.
- [20] COMSOL multiphysics V4.4, [www.comsol.com](http://www.comsol.com).
- [21] MATLAB and statistics toolbox release, The MathWorks, Inc., Natick, Massachusetts, United States, 2012.
- [22] <http://www.omega.com/Temperature/>, visited 29 August, 2016.